Bulletin of the Geological Survey of Japan, vol.56 (7/8), p. 245- 258 , 2005

Paleozoic and Mesozoic granitic rocks in the Hotont area, central Mongolia

Sambuu Oyungerel[1] and Shunso Ishihara[2]

Sambuu Oyungerel and Shunso Ishihara (2005) Paleozoic and Mesozoic granitic rocks in the Hotont area, central Mongolia. *Bull. Geol. Surv. Japan*, vol. 56 (7/8), 245-258, 14 figs, 3 tables.

Abstract: The granitic rocks of the Hotont area were classified into the Late Paleozoic Delgerhaan batholithic complex and Mesozoic Egiindavaa stocks, the latter of which is further divided into normal granitoids and Sn-rich granitoids. The Delgerhaan granitoids are weakly magnetic, their oxygen fugacity being at QMF buffer, while the Egiindavaa granitoids are more reduced belonging generally to ilmenite series. The Sn-rich granites are completely magnetite free and most reduced.

The Delgerhaan granitoids are shoshonitic, whereas the Egiindavaa granitoids are shoshonite to high-K series. Both the granitoids are similar in most of chemical components in the Harker's diagrams, but the Delgerhaan granitoids are richer in P_2O_5 and poorer in Fe_2O_3, TiO_2 and MgO than the Egiindavaa granitoids. Both the granitoids seem to be generated within continental crust in island-arc setting and not fractionated. The Sn-rich granite may be a later intrusion and generated in anorogenic tectonic setting, and well fractionated.

Weak Au-mineralizations are related to the Late Paleozoic Delgerhaan granitic complex. The Late Paleozoic granitoids are too well exposed to have primary base-metal deposits, and the Mesozoic granitoids are not oxidized enough to have base metal mineralizations. Sn and W mineralizations and some Ti-Ta-Nb occurrences are possibly associated with reduced granitoids of the Mesozoic age, particularly with the Sn-rich granites, which may have formed in anorogenic setting.

Keywords: Hotont area, granitoids, Late Paleozoic, Early Mesozoic, chemical compositions, tin granite

1. Introduction

The Hotont area (102° 00'E to 102° 30'E and 47° 10'N to 47° 40'N) is located in Tüvshrüüleh and Hotont sums of Arhangai Aimag in central Mongolia, which is geologically divided into Harhorin and Tsetserleg terranes. The area was mapped at a scale of 1:50,000 by geologists and students of the School of Geology, Mongolian University of Science and Technology (MUST) during the years of 2002 - 2004.

One of the authors (S.O.) visited the area in the 2002 - 2003 field season, and studied the magnetic susceptibility and the mode of occurrence of the granitic rocks. Petrographical description including the modal analyses was later carried out at the laboratories of the MUST. Chemical analyses were performed jointly with the Geological Survey of Japan. In this paper, we report petrographical and chemical characteristics of the granitoids in the Hotont area and discuss mineral resources potentiality of the granitoid affinity.

2. Geologic setting

The Hotont area has been geologically studied by many geologists (Semeikhan and Bold, 1970; Khosbayar *et al.*, 1987; Davaa *et al.*, 1996; Chuluunsüh *et al.*,1996). The area was originally divided into Harhorin uplift block and Hangai Zone. Recently, Chuluun and Javkhlanbold (2004) geotectonically reclassfied the region into Harhorin and Tsetserleg terranes, based upon the terrane map of Mongolia by Tomurtogoo (2004). Geological map of the studied area is given in Fig. 1.

The Harhorin terrane (formerly the Harhorin uplift, e.g., Semeikhan and Bold, 1970) is composed of Lower to Middle Ordovician Hotont Formation (O_{1-2}ht), Lower to Middle Silurian Mongontseej Formation (S_{1-2}mj) and Middle to Upper Silurian Jashil Formation (S_{3-4}jl). The Hotont Formation consists of epidote-chlorite schist, sericite-chlorite schist, muscovite schists and quartzite. The Yashil Formation, which is subdivided into Serven and Hangai Members, is composed of two-mica schists, siltstone and quartzite.

The Tsetserleg terrane is composed of Middle to Upper Devonian Erdenetsogt Formation, Lower Carboniferous Tsetserleg Formation and Upper Carboniferous Jargalant Formation. The Erdenetsogt Formation composed of four members, such as Byanondor, Hanhar, Berh-Uul and Haltaryngozgor, consists of sandstone and siltstone. The Lower Carboniferous

[1] School of Geology, Mongolian University of Science and Technology (MUST)

[2] Geological Survey of Japan, Central 7, 1-1-1 Higashi, Tsukuba, Ibaraki, 305-8567, Japan.

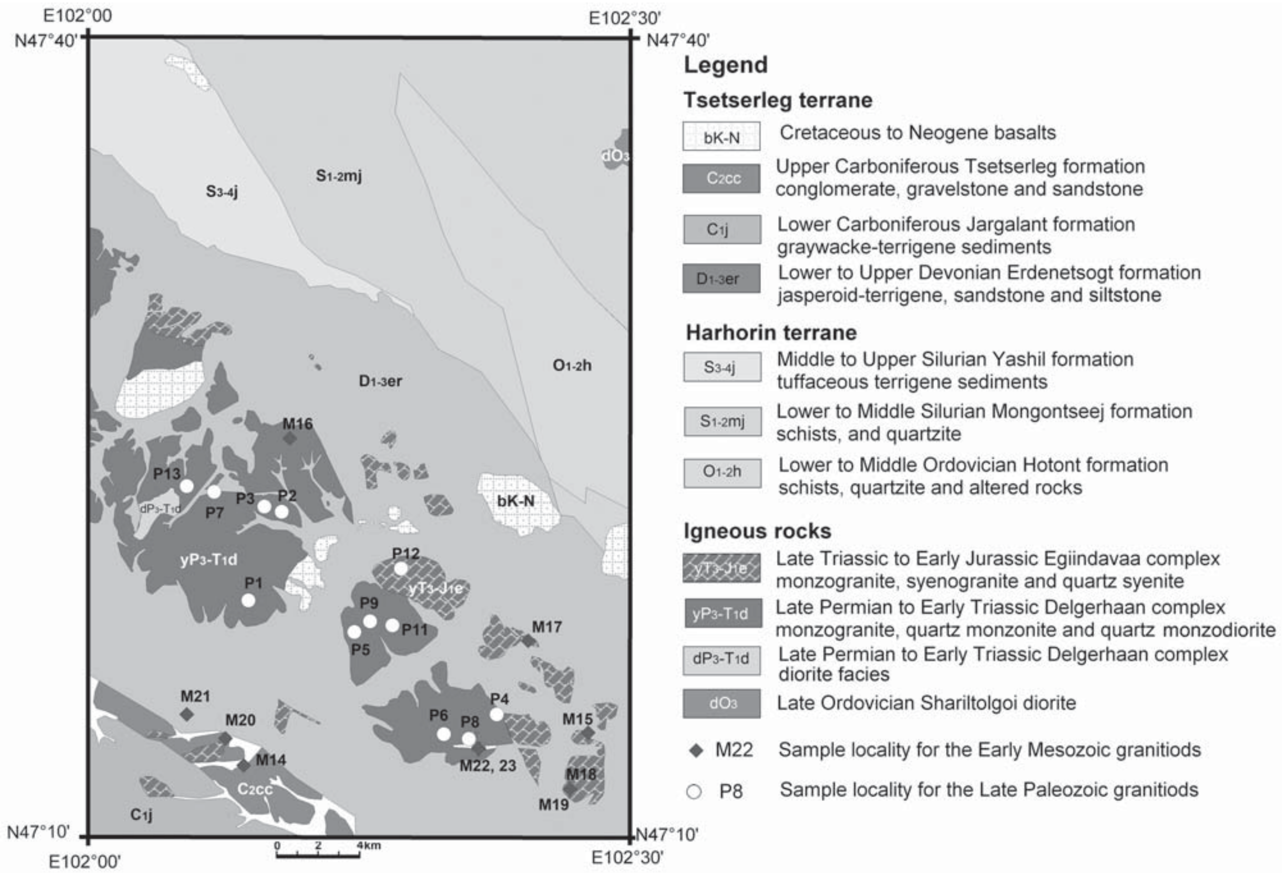

Fig. 1 Geological outline of the studied area and sample localities for the analyzed specimens.

Tsetserleg and Upper Carboniferous Jargalant Formations are mainly composed of conglomerate and sandstone.

An Ordvician dioritic stock (Od_3) occur in the Harhorin terrane. Granitic and minor dioritic rocks intrude abundantly in the sedimentary rocks of the Tsetserleg terrane. By cross-cutting relationship in field, intrusive stage of these granitic rocks must be later than the Carboniferous formations, and is considered as Late Paleozoic and Early Mesozoic in referring to the radiometric age data (e.g., Amar-amgalan, 2004), although we still need additional age determination. Cretaceous to Neogene pyroxene and olivine-pyroxene basalts are distributed mainly in the central part of the Tsetserleg terrane.

3. Geology and petrography of the granitic complexes

The granitic rocks of the Hotont area are divided into Late Paleozoic Delgerhaan complex and Early Mesozoic Egiindavaa complex (Fig. 1). The Delgerhaan granitioids intrude discordantly into the Erdenetsogts sandstones and siltstone of the Middle to Upper Devonian age, and also concordantly into the sediments of the Lower Carboniferous Jargalant Formation and the Upper Carboniferous Tsetserleg Formation. The intrusive age is therefore later than the Upper Carboniferous geologically, and the granitoids are considered intrusion complex of Late Permian to Early Triassic age, based on reconnaissance Rb-Sr isotopic studies of Amar-Amgalan (2004). On the other hand, small stocks of the Egiindavaa granitic complex intrude into the Devonian Erdenetsogt Formation and also into the Late Paleozoic granitoids. The intrusive ages are considered Late Triassic to Early Jurassic (Amar-Amgalan, 2004).

3.1 Delgerhaan granitic complex

This granitic complex occurs along the top and slope of mountains (Fig. 2A) with adomen-like relief. It is a large batholith occupying Tsagduul, Tsohiot, and Tsagaan Asga massifs. The batholith consists mainly of quartz monzodiorite, granodiorite, quartz monzonite and monzogranite (Figs. 3, 4). The mafic silicates are generally biotite with various amounts of hornblende with or without magnetite (Oyungerel and Nyamsuren, 2003).

A number of fine-grained mafic enclaves rich in biotite, 3 cm to 35 cm in size, occur in endocontact zone of the granitoids. Hornfelsic sandstones with schistose textures (Fig. 2B), 10 cm to 1 m in diameter, are also observed in the endocontact zone. A variety of dikes, up to 5 m in the width, occur in the granitoids,

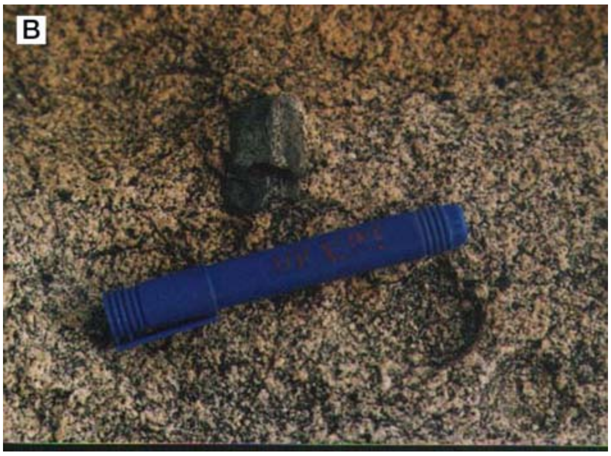

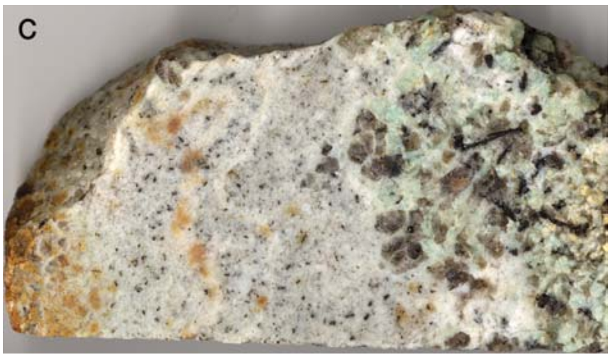

Fig. 2 Field photographs and samples pictures of the Hotont area.
A. Measured outcrop of magnetic susceptibility in field.
B. Sedimentary xenolith at margin of the Late Paleozoic granitoids, Builanttolgoi Mtn. The magnetic susceptibility is low (0.12-0.52 x 10^{-3} SI).
C. Amazonitic Sn-rich granite (right, 23G) and aplite (left, 23A).

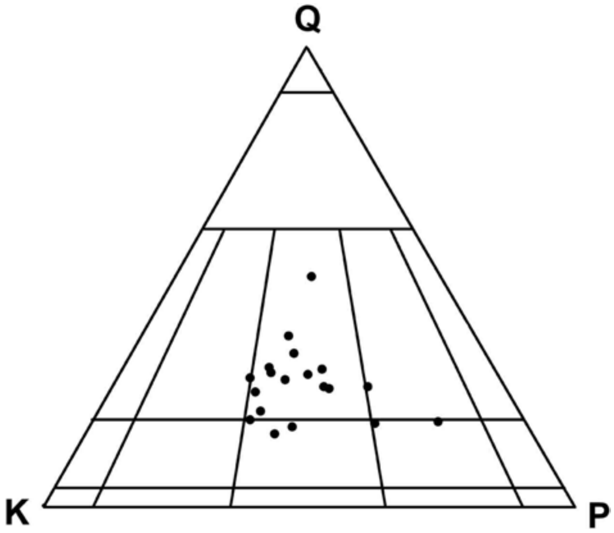

Fig. 3 Plagioclase(P) - K-feldspar(K) - quartz(Q) diagram of the Late Paleozoic granitoids.

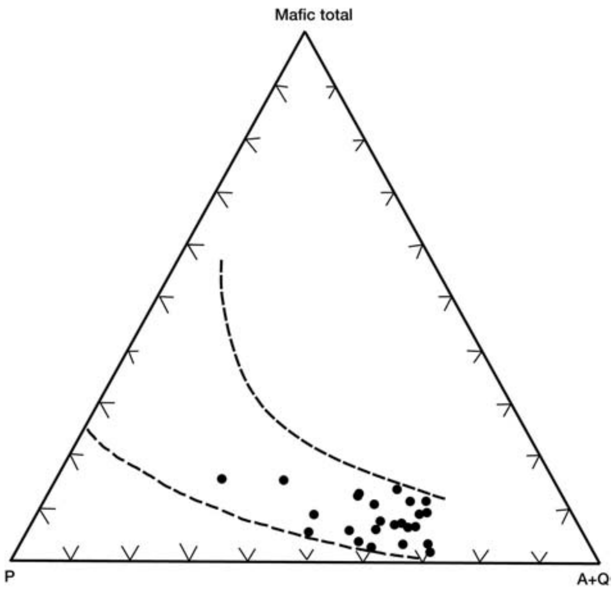

Fig. 4 Mafic total - plagioclase(P) -K-feldspar + quartz(K+Q) diagram of the Late Paleozoic granitoids. The broken line area is for the Japanese Cretaceous granitoids (see Ishihara, 1971).

trending mostly N50 - 70°E. They are diorite porphyrite, black kersantite, hornblende monzodiorite porphyry and pinkish gray quartz monzodiorite porphyry.

Field measurement of magnetic suscetibility by KT-5 Kappameter (Fig. 2A) indicates that the coarse- to medium-grained, biotite quartz monzodiorite (O-26, 102° 17' 21''E, 47° 19' 56''N) range from 4.65 to 12.5 x 10^{-3} SI unit, which is the values of magnetite series (>3.0 x 10^{-3} SI), the medium-grained, biotite-hornblende quartz monzonite (O-71, 102° 22' 89''E, 47° 15' 06''N) varies from 0.03 to 2.39 x10^{-3} SI, which is the values of ilmenite series (<3.0 x 10^{-3} SI). The fine- to medium-grained, hornblende-biotite monzogranite (O-72, 102° 22' 89''E, 47° 14' 63''N) show the magnetic susceptibility of 2.2 - 5.0 x 10^{-3}SI and porphyritic fine- to medium-grained hornblende-bearing biotite monzogranite (O-74, 102° 21' 08''E, 47° 13' 43''N) reveals the magnetic susceptibility of 1.4 -4.5

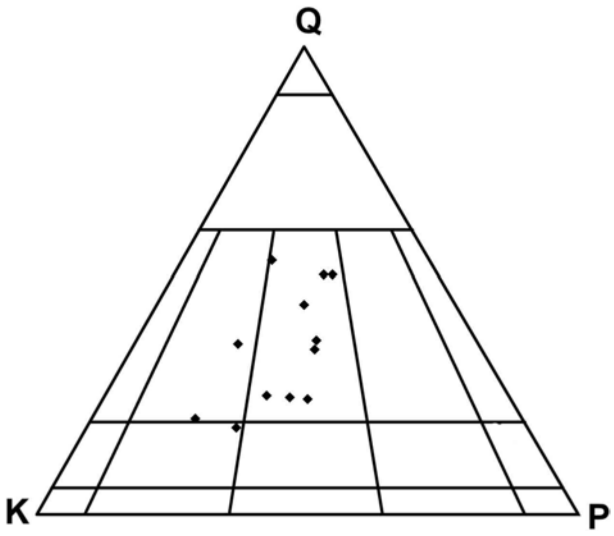

Fig. 5 Plagioclase(P) - K-feldspar(K) - quartz(Q) diagram of the Early Mesozoic granitoids.

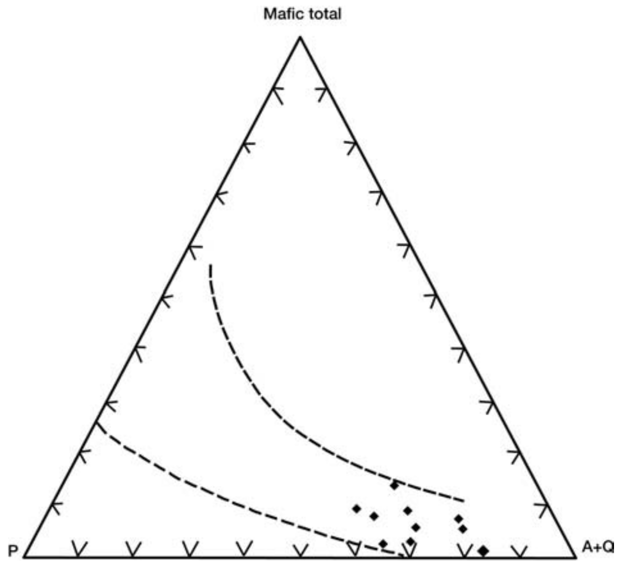

Fig. 6 Mafic total - plagioclase(P) -K-feldspar + quartz(K+Q) diagram of the Early Mesozoic granitoids. The broken line area is for the Japanese Cretaceous granitoids (see Ishihara, 1971).

Table 1 Rock names, localities and magnetic susceptibility of the studied granitoids.

Sample No		Long.	Lat.	Rock name	Magnetic susceptibility
M25	62801	102°21'40	47°13'20	Very fine aplitic granite	0.12 x 10^{-3} SI
M24	62800	102°21'40	47°13'20	Fine-grained muscovite-biotite granite	0.08 x 10^{-3} SI
M23	O23A	102°21'40	47°13'20	Very fine-grained aplitic granite	0.11 x10^{-3}SI
M22	O23G	102°21'40	47°13'20	Fine-grained muscovite-biotite granite	0.06 x 10^{-3} SI
M21	5041	102°05'30	47°14'38	Medium-grained biotite leucogranite	0.12 x 10^{-3} SI
M20	CH36	102°07'38	47°13'44	Medium-grained biotite leucogranite	Not measured
M19	O18A	102°26'44	47°11'50	Weakly cataclasitic fine-to medium-grained granite (slightly weathered)	5.5x10^{-3}SI
M18	O18G	102°26'44	47°11'50	Fine-grained aplitic granite	6.4 x 10^{-3}SI
M17	O69	102°24'25	47°17'24	Porphyritic fine-grained, (hornblende-)biotite quartz syenite	3.3x10^{-3}SI
M16	O54	102°11'13	47°24'59	Pinkish medium-grained, biotite-bearing leucocratic granite	1.8 x 10^{-3}SI
M15	O15	102°27'44	47°13'57	Unequigranular, hornblende-bearing biotite quartz monzodiorite	0.24 x 10^{-3}SI
M14	O48	102°08'39	47°12'43	Porphyritic medium-grained hornblende-biotite granite	2.9 x 10^{-3}SI
P13	O91	102°05'30	47°23'13	Coarse-grained, muscovite-biotite granite	0.14 x 10^{-3}SI
P12	O83	102°17'22	47°20'07	Porphyritic, fine- to medium-grained, hornblende-biotite granite	1.2 x10^{-3}SI
P11	O30	102°16'54	47°17'59	Fine-grained biotite leucocratic granite	0.13x10^{-3}SI
P10	O8	102°51'22	47°01'40	Medium-to coarse-grained (hornblende-)biotite- quartz monzodiorite	1.1 x10^{-3}SI
P9	O81	102°15'39	47°18'08	Fine- to medium-grained, hornblende-biotite granite	0.22 x 10^{-3}SI
P8	O74	102°21'08	47°13'43	Porphyritic fine- to medium-grained, (hornblende-)biotite monzogranite	2.0 x 10^{-3}SI
P7	O90	102°07'01	47°23'00	Cataclasitic, medium-grained, (hornblende-)biotite granite	5.2 x 10^{-3}SI
P6	O76	102°19'47	47°13'56	Fine- to medium-grained, hornblende- biotite granite	1.6x 10^{-3}SI
P5	O33	102°14'47	47°17'44	Fine- to medium-grained (hornblende-)biotite granite	5.1 x 10^{-3}SI
P4	O72	102°22'40	47°14'38	Porphyritic, fine- to medium-grained, (hornblende-)biotite granite	3.1 x 10^{-3}SI
P3	O88	102°09'48	47°22'27	Coarse-grained, hornblende-biotite quartz monzonite	46.8 x 10^{-3}SI
P2	O87	102°10'46	47°22'15	Pinkish, fine- to medium-grained, hornblende-biotite granite	8.6 x 10^{-3}SI
P1	O36	102°08'55	47°18'55	Coarse-grained (hornblende-)biotite quartz monzodiorite (slightly weathered)	0.45 x 10^{-3}SI

x 10^{-3} SI (Oyungerel *et al.*, 2003). Therefore, overall values are intermediate between typical values of the magnetite- and ilmenite-series granitoids.

Rock-forming minerals are represented by plagioclase, K-feldspar, quartz, biotite, sometimes hornblende, opaque minerals, and zircon with various degrees of radioactive haloes and apatite. If primary titanite appears among accessory minerals, its magnetic

Table 2 Chemical compositions of the Late Paleozoic and Early Mesozoic granitoids, Hotont area.

	Late Paleozoic granitoids												
Serial no.	P1	P2	P3	P4	P5	P6	P7	P8	P9	P10	P11	P12	P13
Sample no.	O36	O87	O88	O72	O33	O76	O90	O74	O81	O8	O30	O83	O91
SiO_2	61.83	64.27	64.54	67.99	68.97	69.21	69.33	69.94	70.49	72.03	72.12	72.2	73.49
TiO_2	0.71	0.63	0.6	0.28	0.3	0.27	0.37	0.24	0.26	0.24	0.19	0.14	0.12
Al_2O_3	17.18	16.33	16.8	15.46	15.65	15.55	15.68	15.06	14.93	14.55	14.59	15.27	14.72
Fe_2O_3	5.09	4.32	4.03	2.93	2.84	2.71	2.51	2.42	2.26	1.66	1.62	1.16	0.81
MnO	0.09	0.08	0.08	0.06	0.06	0.06	0.05	0.05	0.05	0.03	0.03	0.01	0.02
Mg0	1.37	1.23	1.14	0.41	0.42	0.37	0.71	0.31	0.42	0.8	0.32	0.2	0.21
CaO	2.84	2.44	2.45	1.28	1.23	0.89	1.72	0.97	1.18	1.63	0.94	0.93	0.63
Na_2O	3.92	4.18	4.63	3.91	4.6	4.73	4.13	4.47	4.22	3.83	3.86	4.27	3.77
K_2O	5.85	4.88	4.82	7.14	5.09	5.29	4.7	5.35	5.04	4.37	5.02	5.04	5.32
P_2O_5	0.43	0.33	0.38	0.22	0.25	0.2	0.2	0.25	0.3	0.08	0.29	0.07	0.08
S	<0.01	0.02	<0.01	0.01	<0.01	0.01	<0.01	0.01	0.01	<0.01	<0.01	0.01	<0.01
LOI	0.66	1.05	0.52	0.39	0.66	0.78	0.57	0.97	0.9	0.82	0.87	0.55	0.86
F	n.d.	n.d.	n.d.	n.d.	n.d.	n.d.	n.d.	n.d.	n.d.	n.d.	n.d.	n.d.	n.d.
Total	99.97	99.76	99.99	100.08	100.07	100.07	99.97	100.04	100.06	100.04	99.85	99.85	100.03
Kai	0.7	8.6	6.8	2	8.7	1.7	5.2	2	0.5	0.8-1.1	1.9	1.2	0.1
Rb	153	189	158	220	217	216	93	217	223	175	218	209	187
Cs	2.9	9.2	7.6	4.4	16.9	25	< 1.5	5.4	31	9.4	19.6	7.9	5.9
Sr	510	408	421	117	182	117	366	115	188	293	182	192	203
Ba	1240	960	1050	223	340	309	1060	293	435	620	424	368	570
Zr	358	361	351	515	335	343	205	309	238	88	155	154	85
Hf	7.3	8.3	8.1	12.1	9.4	9.1	5.7	6.7	9.8	4.5	5.1	6.8	4.4
Nb	12.3	12.8	13.7	22	17.9	16.6	8.8	16.6	15.4	7.1	16	11	8.4
Ta	4.1	2.8	2.0	2.2	3.3	2.1	4.0	1.8	5.6	2.9	2.6	2.9	2.8
Y	25	24	24	30	31	28	21	27	24	9	17	18	9
La	43	46	58	53	58	91	42	67	48	22	27	49	17
Ce	94	97	120	152	122	161	84	133	88	43	56	87	29
V	42	44	33	5	11	4	26	9	11	12	5	<3	<3
Cr	39	21	38	17	15	22	23	31	38	34	21	15	11
Co	<8	<7	<7	<6	<6	<6	<5	<5	<5	6	<5	5	4
Ni	6.4	6.0	5.5	<2	1.5	<2	1.0	<2	2.1	7.4	2.0	2.5	3.9
Cu	7.9	5.3	3.0	0.7	< 0.5	< 0.5	< 0.5	0.7	< 0.6	< 0.4	< 0.4	1.0	1.1
Zn	73	76	70	40	68	63	53	63	55	28	35	16	18
Pb	36	36	35	32	42	40	29	42	42	40	38	28	40
Ga	20.7	19.9	20.5	21.1	21.1	20.7	16.9	20.4	19.1	16.0	18.7	18.6	16.6
Ge	1.0	1.1	1.1	1.4	1.5	1.3	1.4	1.2	1.0	1.3	1.4	1.3	1.2
As	0.5	5.7	4.4	15.6	19.4	5.5	0.9	8.1	9.7	7.8	7.1	5.1	0.7
Se	0.3	0.5	0.6	0.3	0.2	0.6	0.3	0.3	0.6	0.5	0.5	0.5	0.4
Mo	2.1	0.7	0.3	0.8	2.1	0.2	1.4	0.4	1.0	< 0.2	2.8	0.6	0.6
W	0.9	<2	<2	2.4	2.1	2.5	<2	1.3	5.7	2.2	28	2.9	1.8
Sn	2.9	3.6	3.0	3.3	5.8	5.4	2.3	4.2	8.0	1.8	4.1	3.4	1.8
Cd	< 0.2	< 0.2	< 0.2	< 0.2	< 0.2	< 0.2	< 0.2	0.2	< 0.2	< 0.2	< 0.2	< 0.2	< 0.2
Tl	2.1	2.5	2.5	2.5	2.9	2.6	1.4	2.7	3.2	2.5	2.6	2.7	2.0
Sb	< 0.5	0.6	< 0.5	1.3	1.3	1.4	< 0.5	0.8	1.6	0.8	< 0.5	0.5	< 0.5
Bi	< 0.4	0.9	0.7	0.7	0.8	1.2	0.6	0.5	1.5	1.3	8.6	0.5	0.4
Th	19.6	26	20	40	30	35	19.4	27	35	24	27	39	18.4
U	1.5	1.3	1.3	2.9	4.0	2.6	0.4	3.1	4.9	4.3	9.9	2.4	0.6
ASI	0.96	0.98	0.97	0.94	1.02	1.03	1.04	1.01	1.03	1.04	1.08	1.08	1.12
K_2O+Na_2O	9.77	9.06	9.45	11.05	9.69	10.02	8.83	9.82	9.26	8.20	8.88	9.31	9.09
K_2O/Na_2O	1.49	1.17	1.04	1.83	1.11	1.12	1.14	1.20	1.19	1.14	1.30	1.18	1.41
Rb/Sr	0.30	0.46	0.38	1.88	1.19	1.85	0.25	1.89	1.19	0.60	1.20	1.09	0.92

Kai; magnetic susceptibility x 10^{-3}, SI unit. Analysts: B. W. Chappell, GEOMOC. F(ISE) by Actlabs. Ltd.

susceptibility is usually high, and the rock belongs to magnetite-series.

Modal analyses indicate that granitoids of the Delgerhaan complex are plotted mostly in the monzogranite field and some plotted in the quartz monzogranite and quartz monzodiorite field (Fig. 3). Contents of the mafic minerals are generally low (Fig. 4) but vary from 1.2 to 18.0 %. Panning of the stream sediments at Tagtolgoi Au-occurrence indicates magnetite contents of 90 - 200 grams/ton and ilmenite contents of 30 - 70 grams/ton, implying both magnetite and ilmenite are contained in the original granitoids.The chemical compositions are given in Tables 2 and 3.

3.2Egiindavaa granite complex

The Egiindavaa granitic complexes occur as stock-like small bodies controlled by deep faults with north-

Table 2 (continued).

	Early Mesozoic granitoids											
Serial no.	M14	M15	M16	M17	M18	M19	M20	M21	M22	M23	M24	M25
Sample no.	O48	O15	O54	O69	O18G	O18A	CH36	5041	O23A	O23G	62801	62800
SiO_2	66.1	70.1	71.89	72.22	75.19	68.17	76.32	77.35	76.23	77.91	74.6	77.15
TiO_2	0.55	0.28	0.2	0.23	0.11	0.46	0.14	0.1	<0.01	0.03	0.16	0.02
Al_2O_3	15.74	15.58	14.42	14.27	13.18	15.48	13.23	12.69	13.81	11.66	13.85	12.76
Fe_2O_3	3.53	2.2	1.72	1.99	1.13	3.21	1	0.63	0.4	1.19	1.12	0.75
MnO	0.07	0.05	0.04	0.05	0.02	0.05	0.07	0.01	0.03	0.09	0.05	0.02
Mg0	1.13	0.67	0.18	0.47	0.21	1.66	0.3	0.11	0.02	0.02	0.2	0.03
CaO	2.39	1.62	0.47	1.08	0.65	2.44	0.84	0.31	0.18	0.11	0.84	0.16
Na_2O	4.2	4.14	4.29	4.38	3.59	3.73	4.37	4.31	6.43	3.08	3.97	4.18
K_2O	4.4	4.17	5.62	4.37	5.1	4.34	3.26	4.01	2.64	5.41	5.04	4.59
P_2O_5	0.49	0.14	0.26	0.1	0.05	0.16	0.05	0.04	0.03	0.04	0.07	0.05
S	0.05	<0.01	<0.01	<0.01	<0.01	<0.01	<0.01	<0.01	<0.01	<0.01	<0.01	<0.01
LOI	1.1	1.05	0.74	0.65	0.64	0.34	0.47	0.41	0.17	0.33	0.19	0.19
F	n.d.	n.d.	n.d.	n.d.	0.03	0.01	n.d.	n.d.	0.14	0.27	0.12	0.39
Total	99.75	100	99.83	99.81	99.87	100.04	100.05	99.97	99.94	99.87	100.09	99.9
Kai	2.9-3.9	0.24	1.84	6.2	6.4	5.5	2.99	0.1	<0.1	<0.1	<0.1	<0.1
Rb	201	192	92	133	134	171	98	58	510	930	298	1150
Cs	12.3	12.1	2.1	3.5	7.5	5.9	4.2	5.1	48	89	14.0	28
Sr	389	370	103	181	300	86	88	7.5	5.4	5.9	104	3.9
Ba	760	670	570	496	770	173	550	1430	8.2	28	246	<2
Zr	262	147	228	163	127	96	65	62	61	142	93	124
Hf	6.0	4.2	6.6	5.9	4.4	4.3	3.0	3.0	12.2	12.4	3.4	19.2
Nb	13.2	9.4	5.6	11.2	9.6	8.9	7.6	2.5	12.5	67	21	58
Ta	<2	2.5	1.4	2.7	3.0	2.8	1.1	<2	3.6	4.0	5.1	15.4
Y	23	16	14	23	15	10	23	12	67	85	19	108
La	61	33	131	50	34	31	14	5	8	5	35	17
Ce	122	70	229	88	54	37	29	16	34	23	63	50
V	31	52	<3	13	17	7	<3	<3	3	3	4	<3
Cr	45	63	26	34	22	29	24	16	23	18	39	12
Co	<7	<7	<4	<5	5	<4	3	3	<2	7	4	6
Ni	6.2	14.7	<2	0.6	1.9	0.7	<2	0.4	2.2	1.6	1.3	3.8
Cu	5.1	1.9	< 0.4	< 0.5	< 0.5	< 0.4	< 0.4	< 0.3	< 0.5	< 0.6	< 0.4	< 0.8
Zn	63	46	43	49	43	20	24	17	49	158	40	282
Pb	34	34	29	31	36	46	19.1	19.9	96	116	50	131
Ga	20.4	17.1	16.9	17.2	16.6	16.0	14.1	10.8	36.3	25.4	21.6	43.2
Ge	1.3	1.3	0.8	1.1	1.1	1.3	1.9	1.2	2.9	1.9	1.7	4.1
As	10.1	3.7	0.5	7.0	2.1	2.7	< 0.4	< 0.4	2.1	6.7	1.8	4.7
Se	0.3	0.4	0.3	0.4	0.3	0.2	0.3	0.3	0.5	0.7	0.4	0.5
Mo	1.6	1.2	1.0	0.3	0.6	< 0.2	1.3	< 0.2	< 0.2	< 0.2	< 0.2	< 0.2
W	5.2	<2	1.0	1.8	1.8	3.0	2.5	2.1	4.0	4.5	2.9	5.8
Sn	4.9	2.6	1.3	2.3	3.0	1.3	1.6	0.7	7.6	22	6.7	158
Cd	< 0.2	0.2	< 0.2	< 0.2	< 0.2	< 0.2	< 0.2	< 0.2	< 0.2	< 0.2	< 0.2	< 0.2
Tl	2.3	2.2	1.5	1.6	2.5	2.0	1.5	1.3	3.3	6.6	2.3	7.4
Sb	1.2	0.4	< 0.5	< 0.5	0.4	< 0.5	< 0.5	0.5	0.9	0.6	< 0.5	0.6
Bi	1.1	0.4	0.7	0.4	0.7	0.9	0.7	0.5	7.3	11.7	0.4	2.8
Th	55	29	26	22	20	37	5.3	5.3	25	49	37	34
U	6.6	2.6	1.1	3.7	< 0.5	2.0	< 0.5	< 0.5	3.6	6.7	20	< 0.5
ASI	0.98	1.09	1.03	1.03	1.05	1.01	1.08	1.06	1.00	1.05	1.02	1.05
K_2O+Na_2O	8.60	8.31	9.91	8.75	8.69	8.07	7.63	8.32	9.07	8.49	9.01	8.77
K_2O/Na_2O	1.05	1.01	1.31	1.00	1.42	1.16	0.75	0.93	0.41	1.76	1.27	1.10
Rb/Sr	0.52	0.52	0.89	0.73	0.45	1.99	1.11	7.73	94.44	157.63	2.87	294.87

Kai; magnetic susceptibility x 10^{-3}, SI unit. Analysts: B. W. Chappell, GEOMOC, and Actlabs. Ltd.

easterly trends. They show strongly sheared and slightly weathered outcrops caused by recent uplifting and NW - SE shearing along the Harhorin and Hanhar faults. Therefore it is difficult to obtain fresh rock samples for geochemical studies.

The Egiindavaa granites are granodiorite to monzogranite (Figs. 5, 6), containing biotite universally and some hornblende as major mafic silicates, which may be enriched in endogranitic zone when the bulk composition is granodioritic. Mafic enclaves are rare. There occur a few dikes of granite-pegmatite, aplite, biotite syenite porphyry and amazonite porphyry. The chemical compositions are given in Tables 2 and 3.

At one place near the Tsagduul massif, fine to medium grained mica granites with green amazonitic K-feldspar and dark quartz (Fig. 2C) occur in the Delgerhaan batholith. These rocks may be a later, early

Table 3 Trace element and REE compositions of selected granitoids from the Hotont area.

Age	Paleozoic granitoids		Mesozoic granitoids		Sn-rich granite	
Sample no.	P3	P13	M14	M18	M24	M25
V	30	-5	34	18	7	-5
Co	5	1	5	3	-1	-1
Zn	45	-30	38	-30	38	197
Ga	21	19	23	19	23	47
Ge	1.2	1.1	1.2	1.1	1.7	3.4
Rb	153	190	210	137	294	1,120
Sr	388	194	384	284	99	2
Zr	420	88	368	177	103	174
Nb	14.7	8.9	15.9	10.0	21.5	65.3
Sn	3	2	5	3	6	147
Cs	5.8	7.1	13.9	7.6	14.5	29.5
Ba	1,090	595	823	808	265	-3
La	61.6	22.0	69.0	38.7	34.9	16.6
Ce	127.0	37.6	136.0	61.5	67.0	48.7
Pr	13.90	4.31	14.90	7.52	7.01	5.98
Nd	50.3	15.4	52.6	25.8	24.2	25.2
Sm	8.87	2.97	8.74	4.16	4.24	7.05
Eu	1.680	0.582	1.450	0.689	0.523	0.006
LREE	263.35	82.65	282.69	138.37	137.87	103.54
Gd	6.65	2.33	6.33	3.29	3.20	7.38
Tb	0.95	0.35	0.94	0.49	0.52	1.97
Dy	4.91	1.81	4.76	2.57	2.92	15.70
Ho	0.93	0.32	0.88	0.53	0.60	3.84
Er	2.75	0.92	2.68	1.64	2.00	14.40
Tm	0.413	0.137	0.415	0.274	0.360	2.990
Yb	2.57	0.86	2.69	1.81	2.59	22.60
Lu	0.377	0.124	0.395	0.280	0.435	3.350
Y	27.1	10.5	28.6	17.2	21.8	116.0
HREE	46.62	17.35	47.69	34.65	34.43	188.23
Hf	11.1	3.0	9.9	5.2	4.2	21.6
Ta	1.3	2.0	1.6	1.2	3.9	17.6
W	1.1	-0.5	1.5	0.9	2.4	1.5
Tl	1.0	0.8	0.9	0.7	1.6	5.9
Pb	31	44	26	30	41	104
Bi	0.2	0.1	0.7	1.1	0.4	3.8
Th	21	20.2	52.6	20.7	33.8	37.5
U	3.4	2.5	7.6	2.7	21.8	8.3
REE total	309.97	100.00	330.38	174.02	172.30	291.77
Rb/Sr	0.39	0.98	0.55	0.48	3	560
Sr/Y	15.5	18.5	13.4	16.5	4.5	0.02
La/Yb	24.0	25.6	25.7	21.4	13.5	0.7
LREE/HREE	5.7	4.8	5.9	4.0	4.0	0.55

Analyst: Actlabs, Ltd. (ICP-MS)

Mesozoic intrusion, although the field relationship is ambigous for the poor exposure. The granites are very high in the trace amounts of tin (see geochemistry chapter), and therefore called tentatively Sn-rich granites in this paper.

Field measurement of magnetic susceptibility on the representative rock types are as follows: coarse- to medium-grained, biotite quartz syenite (O-63, 102°13' 50''E, 47°24' 50''N ranging from 1.14 up to 2.29 x 10^{-3}SI; hornblende-bearing biotite qaurtz syenite (O-69, 102°24' 50"E, 47°17' 24"N) measured at 2.89, 3.37, 3.71 x 10^{-3} SI; fine- to medium-grained, two-mica, leucocratic monzogranite (O-16, 102° 26' 25''E, 47° 12' 50''N) with low values as 0.47, 0.34, 0.44, 0.36 x 10^{-3} SI; medium-grained, biotite-bearing monzogranite (O-56, 102° 06' 51''E, 47° 26' 05''N) with 0.44 - 2.11 x 10^{-3} SI, and cataclasitic, coarse-grained, biotite-bearing syenogranite (O-66; 102° 26' 372''E, 47° 15' 533''N) with magnetic susceptibility of 0.11 - 0.27 x 10^{-3} SI).

The Mesozoic granitoids are therefore composed mostly of ilmenite series, represented by either biotite or biotite-muscovite assemblages, which are common in Sn-mineralized terrains, such as Japan and Malay Peninsula (Ishihara, 1977; Ishihara *et al.* 1979). Only some hornblende-bearing phase of the Egiindavaa complex belongs to mgnetite series. The Sn-rich granite seems to be most reduced granite in the Hotont area.

Rock-forming minerals of the Egiindavaa complex are K-feldspar, plagioclase, quartz, biotite, rarely hornblende, opaque minerals, radiogenic zircon and apatite. By modal analyses, the granitoids are mostly plotted in monzogranite and syenogranite-quartz syenogranite fields (Fig. 5) Contents of the mafic minerals are generally low varying from 0.8 to 10.0 % (Fig. 6). Therefore, granitoids of the Egiindavaa complex are more leucocratic and alkaline than those of the Delgerhaan complex.

3.3 Sn-rich granite

This granite, containing pale green color K-feldspar (amazonite, Fig. 2C), is found in a prospecting shaft of Ulaanbulaag valley near the Tsagduul massif of the Late Paleozoic Delgerhaan complex. This is so different from the other rocks that they may belong to younger, Mesozoic age. The quartz is dark transparent which is due to radioactive decay. The biotite is platy crystals and is really black in color, indicating Fe^{2+}-rich variety, because of lack of magnetite shown by very low degree of the magnetic susceptibility (less than 0.1 x 10^{-3} SI). The rocks are so different from the surrounding granodiorite and the chemistry is also clearly different as mentioned later, and are therefore considered as a Mesozoic stock intruded into the Late Paleozoic granitoids.

The granite consists of microcline (45 - 50%), plagioclase (20 - 25%), quartz (25 - 30%) and biotite (2 - 3%) with small amounts of opaque minerals. Microcline is anhedal and it shows grid twinning. Microcline is partly corroded by quartz. Albite rim is developed along contact with the microcline. The plagiocalse is euhedral to subhedral, and shows polysynthetic twinnings. The anorthite contents are 8 - 10 %. Plagioclase is sometimes replaced by microcline. Biotite is subhedral and includes accessory minerals of apatite, radioactive zircon and opaque minerals. Quartz microveinlets, 0.04 - 0.4 mm wide, may be seen in the granite.

4. Mineralizations in the Hotont area

In the Hotont area, Tagtolgoi (102°00' 43''N, 47°26' 55E) and Baahanbulag (102°12' 17''N, 47°25' 53''E) Au-occurrences, and Hanhar (102°03' 29''N, 47°28' 22E), Namdavaa (102° 10' 55''N, 47° 14' 09''E) and Baruunganga Au-mineralized points (102° 01' 37''N, 47°24' 54E) are found in the Late Paleozoic Delgerhaan complex, which is weakly magnetic and can be an intermediate series of Ishihara *et al.* (1984). Gold mineralizations with similar oxidation state have been reported in eastern Australia (Blevin, 2004).

On the contrary, the Egiindavaa granitoids are associated with tin-tungsten mineralizations, e.g., Ulaanbulag tin-mineralized point (102°22' 22''N, 47° 16' 38''E), Tomorhairhan Sn-W occurrence (102° 03' 34''N, 47° 12' 07E), Tömört scheelite (W)-occurrence (102° 05' 12'') and Ulaanbulag Ti-Ta-Nb placer occurrence (102° 21' 22''N, 47° 13' 52''E). Within the Sn-rich granitic body, there occur cassiterite-greisen meneralizations, and cassiterite is also found in the stream sediments in this area.

This spatial relationship between the ilmenite-series granitoids and Sn-W mineralizations is widely recognized in the other Phanerozoic terrains of the Circum-Pacific region (Ishihara, 1977).

.

5. Geochemistry of the granitoids

Chemical analyses were made on representative samples from the Paleozoic Delgerhaan complex (P1-13, 13 samples) and the Mesozoic Egiindavaa granitoids (M14 - 25, 12 samples). Their localities are given in Table 1 and Fig. 1, and the results are listed in Tables 2 and 3. The Mesozoic granitoids are divided into normal granitoids (M14 - 21) with Sn contents of 0.7 - 4.9 ppm and Sn-rich granite (M22 - M25) with Sn contents of 6.7 - 1,158 ppm. The analytical results are plotted with these cateories in the Harker's diagrams of Figs. 7 to 12.

5.1 Feldspar components

Al_2O_3 contents decrease with increasing of SiO_2 (Fig. 7),

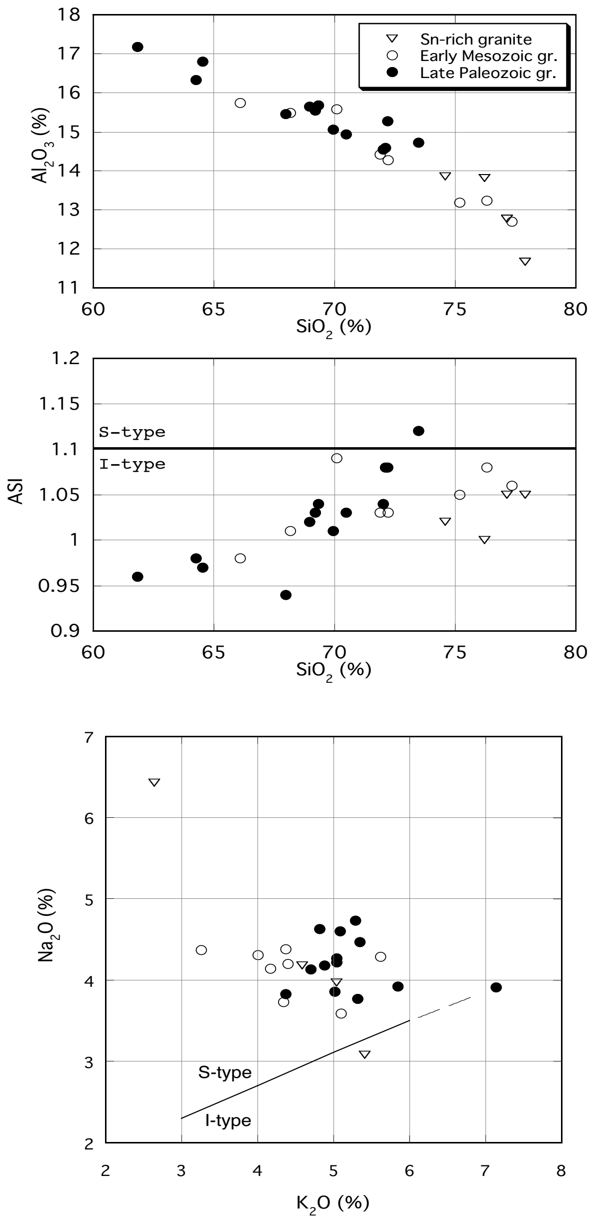

Fig. 7 Harker diagrams for Al_2O_3 and ASI (Zen, 1992), and Na_2O vs. K_2O. S- and I-type division from Chappell and White (1974).

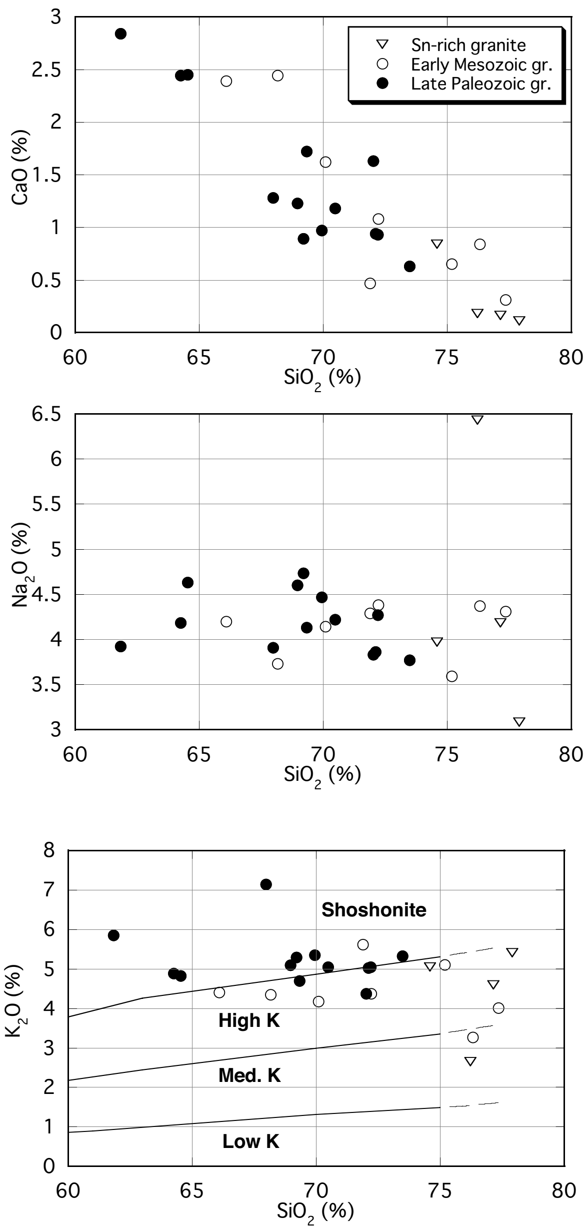

Fig. 8 Harker diagrams for CaO, Na_2O and K_2O.

and Mesozoic granitoids have the least amount of Al_2O_3, because they are rich in SiO_2. However, the alumina saturation index (ASI, Zen, 1992) of both Paleozoic and Mesozoic granitoids is mostly above 1.0, i.e., peraluminous, but below 1.1, implying all the rocks belong to I type of Chappell and White (1974). In the Na_2O vs. K_2O diagram, all the granitoids are also plotted in the I-type field (Fig. 7).

In the K_2O-SiO_2 diagram, most of the Paleozoic granitoids are plotted in the shoshonite field, but the Mesozoic granitoids are plotted in both the shoshonite and high-K calc-alkaline-series field (Fig. 8). Na_2O contents are generally higher in the Paleozoic granitoids than in the Mesozoic granitoids. Very high value of the O23A Sn-rich granite (6.4 % Na_2O) may be due to late magmatic albitization.

The total alkali contents are high in the Paleozoic granitoids, being 8.2 - 11.1% Na_2O+ K_2O, but their Rb/Sr ratios are low ranging from 0.3 to 1.9, implying that they are not fractionated before the emplacement. The Mesozoic granitoids have also low ratios of 0.5 - 2.0, except for the M21 granite with the Rb/Sr of 7.7. Therefore, these granitoids have disadvantage in concentrating the metals associated with magmatic fractionation, such as Mo and Pb-Zn.

The Sn-rich granites are high in Rb (Fig. 9), Rb^+(1.57A) is larger than K^+(1.46A), thus substituting K^+ of K-bearing minerals in a late crystallizing

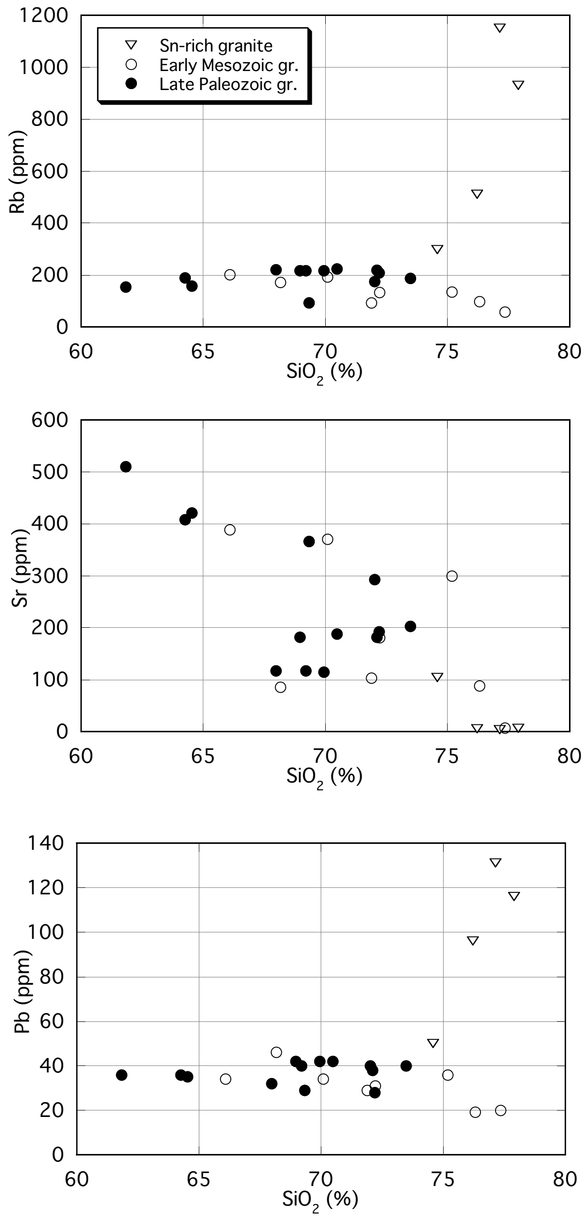

Fig. 9 Harker diagrams for Rb, Sr and Pb.

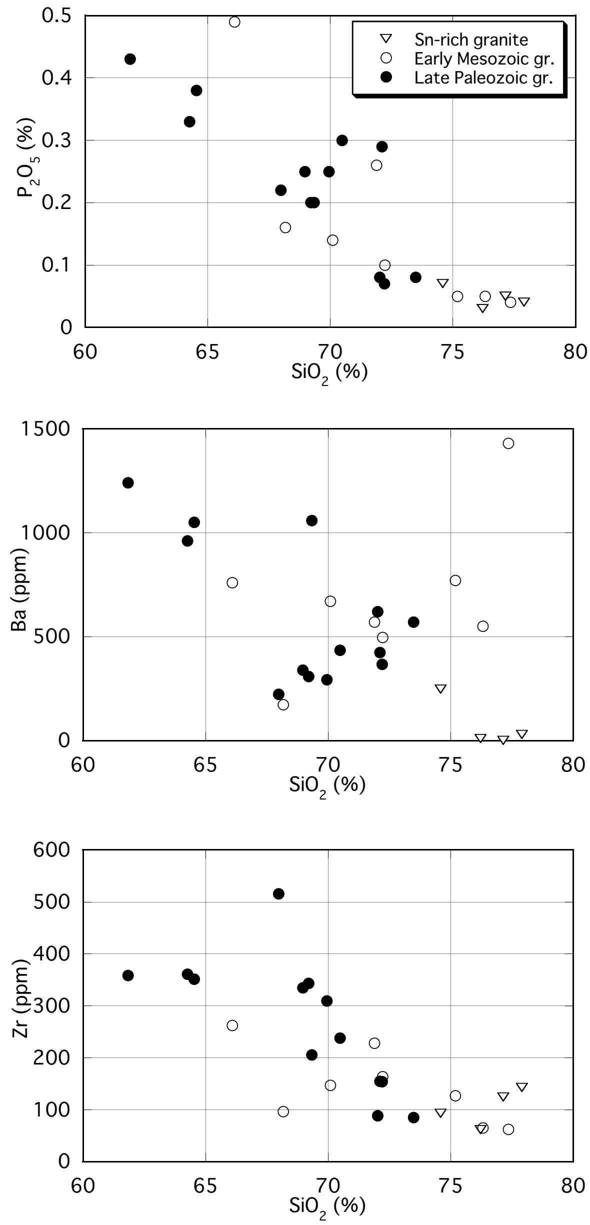

Fig. 10 Harker diagrams for P_2O_5, Ba and Zr.

stage for the larger ionic size. The Sn-rich granite must be also high in Pb^{2+}(1.02A), which is expected to substitute K position in an early crystallizing stage for the smaller ionic radius and higher electron charge. These granites are also high in Cs^{+}(1.78A), which may be concentrated in the latest phase of K-feldspar.

Ba^{2+}(1.44A), replacing an early crystallized K-bearing minerals, is generally abundant in low SiO_2 rocks, but the contents are very variable on the early Mesozoic granites (Fig. 10). Some of the high SiO_2 granites are very high being over 1,000 ppm, but the Sn-rich granites are less than 28 ppm (Table 2).

Ga, not shown in Fig. 10 and replacing Al_2O_3 in feldspars, is generally higher than 20 ppm in A-type granite (Collins *et al.*, 1988). Here the element is below 21 ppm for most of the rocks (Table 2), except the Sn-rich granites which vary from 22 to 43 ppm. Zr is higher in the Paleozoic granitoids than in the Mesozoic granitoids (Fig. 10).

5.2 Mafic components

The Harker diagrams (Fig. 11) indicate that the Paleozoic granitoids are plotted generally lower than the Mesozoic granitoids in the total Fe_2O_3, TiO_2 and MgO. MgO is less than 1.7% throughout the granitoids implying a little or no mantle components involved in these granitoids.

Vanadium is low, below 52 ppm (Table 2). The element (V^{2+}0.87A; V^{3+}072A) may substitute Fe^{2+} (0.71A)

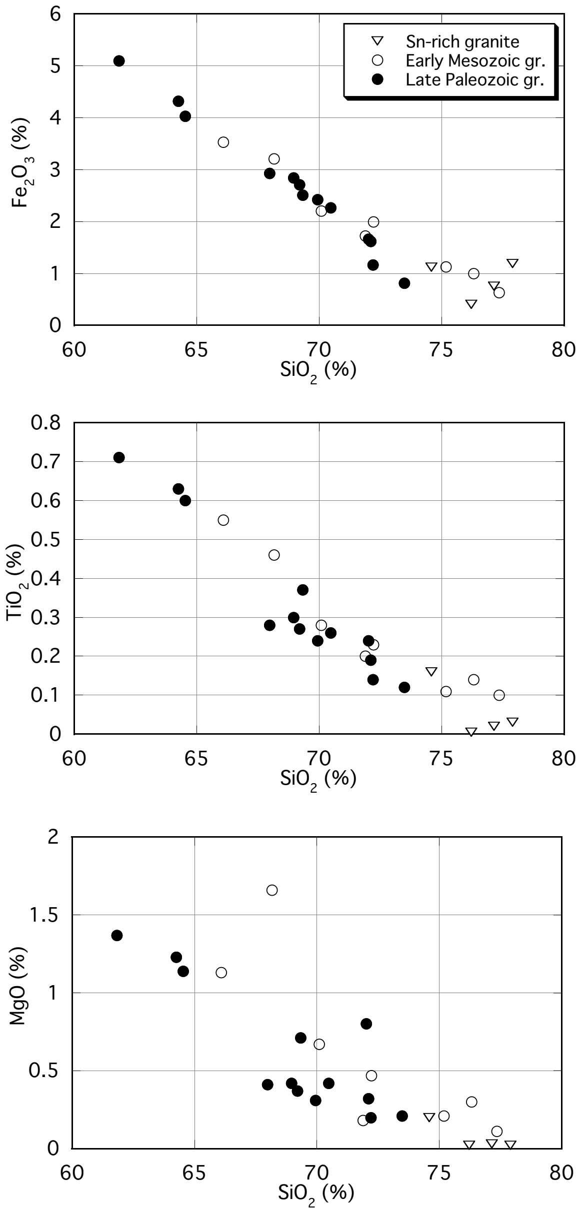

Fig. 11 Harker diagrams for Fe_2O_3, TiO_2 and MgO.

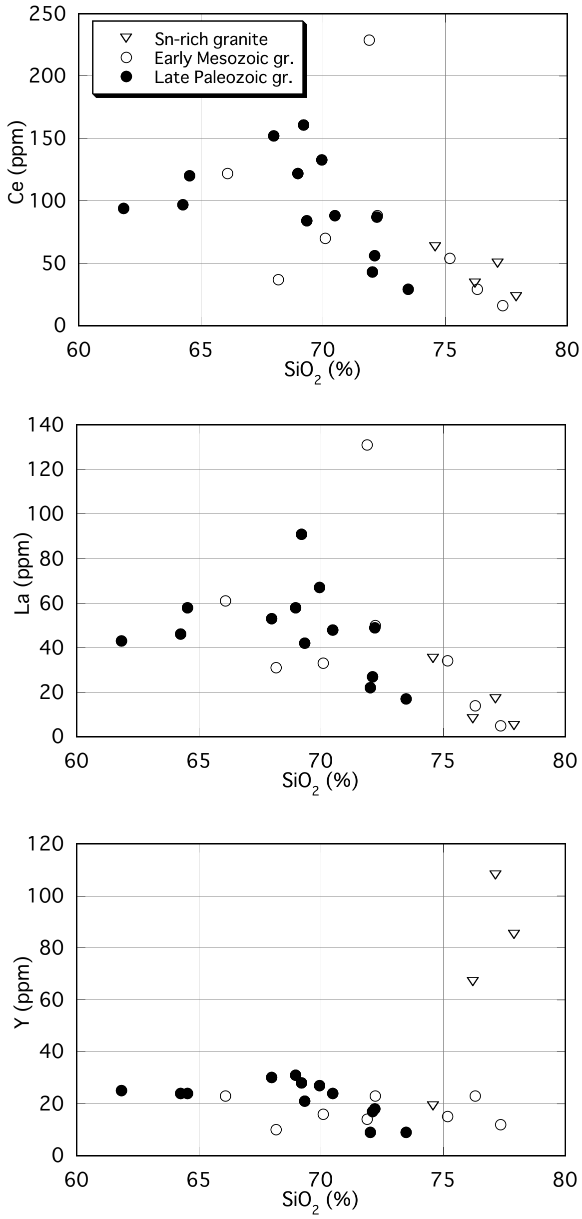

Fig. 12 Harker diagrams for Ce, La and Y.

and Fe^{3+} (0.57A) of rock-forming magnetite. Chromium (Cr^{2+}0.81 A; Cr^{3+}0.70A, Cr^{4+}0.52A) and Zn^{2+} (0.68A) may replace iron in the rock-forming silicate. P_2O_5 contents are more in the Paleozoic granitoids than in the Mesozoic granitoids (Fig. 10). There is no microscopic evidence of monazite occurring in the Paleozoic granitoids; thus the element must be present as apatite. The Paleozoic granitoids are richer in apatite than the Mesozoic granitoids.

Nb is less than 18 ppm in the normal granitoids but high as 13 - 67 ppm in the Sn-rich granite. Ta is lower than 6 ppm in most granitoids but high in the Sn-rich granite as 4 - 15 ppm. Y is much higher in the Sn-rich granite (19 - 108 ppm) than the normal granites (9 - 31 ppm, Table 2).

5.3 REE components

REE components are analyzed by ICP-MS method on representative samples and listed in Table 3. The Paleozoic granitoids have the total REE of 100 and 310 ppm, and the Mesozoic granitoids of 174 and 330 ppm. The Sn-rich granites have lower values as 172 and 292 ppm, but the Rb-rich granite of the sample M25 has the lowest LREE/HREE ratio, implying this rock is very rich in HREE (e.g., La/Yb ratio=0.74), with a typical bird-flying REE pattern (Fig. 13).

On the chondrite normalized REE patterns (Fig. 13), the studied granitoids show similar patterns, high in LREE but low in HREE with weak Eu negative anomalies, except for one of the Sn-rich granites. The granodiorite P3 of the Paleozoic Delgerhaan granitoids is

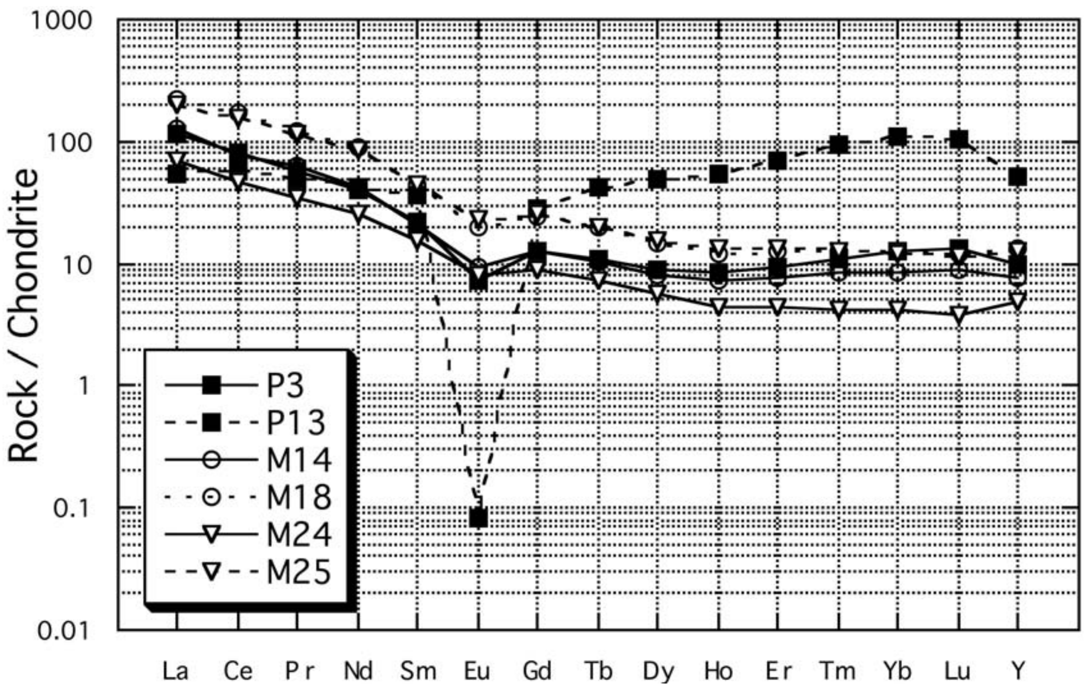

Fig. 13 Chondrite normalized REE pattern of the representative granitoids from the Hotont area.

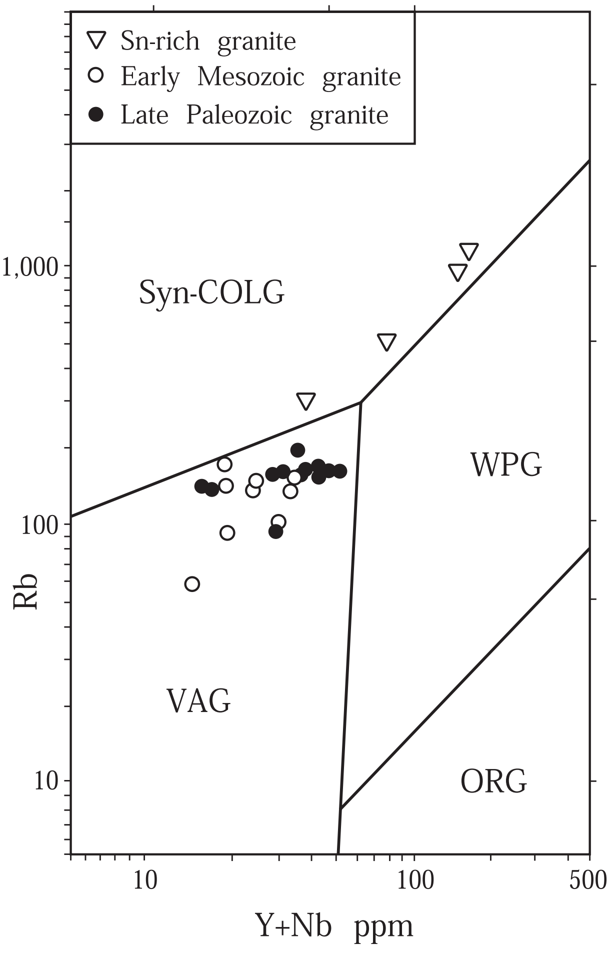

Fig. 14 The studied granitoids in the Rb vs. Y+Nb discrimination diagram (Pearce *et al*., 1984).

richest in REE and the granite P13 is least in REE. Among the Mesozoic Egiindavaa complex, the granodiorite M14 and the granite M18 are plotted between the two values.

The Sn-rich aplitic granite M24 has strong concentration of HREE, which may be contained in accessory minerals. Eu is strongly depleted, which is due to plagioclase fractionation. This aplitic granite should be formed from the final fractional melt of the Sn-rich granites.

5.4 Discrimination diagrams

The analytical data are plotted in the discrimination diagram of Pearce *et al*. (1984). Almost all the granitoids are plotted in the uppermost part of the volcanic arc granites (VAG), except for the Sn-rich granites, which are plotted in the syn-collisional granite field (syn-COLG) , because of the high contents of Rb (Fig. 14). No granitoids are plotted in the within-plate granite field (WPG), although three of the Sn-rich granites are plotted in the WPG field of the Nb-Y diagram, which is not shown here. Therefore, most of the granitoids are considered generated under an island-arc setting.

The Sn-rich granites are high in F, Rb, Cs, Nb, Ta, Y, Zn, Pb, Ga and Sn, which are characteristics of anorogenic (A-type) granites. The Sn-rich granites may have been originated locally along structural weakness within the continental crust. These anatectic melts may have possibly intruded as a younger small stock in the Late Paleozoic granitoids.

6. Concluding Remarks

The granitic rocks of the Hotont area, composed of the Late Paleozoic Delgerhaan batholithic complex and Mesozoic Egiindavaa stocks, are mostly biotite monzogranite and some hornblende-biotite granodiorite, associated with little mafic rocks. The Delgerhaan granitoids contain generally small amounts of magnetite, and can be considered crystallization around the QMF buffur. The Egiindavaa granitoids are more reduced belonging mostly to ilmenite series, thus they can be formed below the NNO buffer (Ishihara, 1977). The Sn-rich granites are completely magnetite free and most reduced.

The Delgerhaan granitoids are shoshonitic, whereas the Egiindavaa granitoids are shoshonite to high-K series. Both the granitoids are similar in most of chemical components in the Harker's diagrams, but the Delgerhaan granitoids are richer in P_2O_5 and poorer in Fe_2O_3, TiO_2 and MgO than the Egiindavaa granitoids. Both the granitoids seem to be generated within continental crust with K-rich I-type sources under an island-arc setting.

The Sn-rich granites are high in F, Rb, Cs, Nb, Y, Zn, Pb, Ga and Sn, which are characteristics of A-type granites. They may be a Mesozoic intrusion and generated in anorogenic tectonic setting. The granites should have been formed by remelting of an older reduced granitic materials in anorogenic environment, and carried Sn and rare metal mineralizations.

The Delgerhaan granitoids are too well exposed to have metallic mineral deposits, which tend to occur generally associated with small plugs or stocks. The granitoids are not oxidized enough to concentrate sulfur-combined ore minerals. Placer gold and weak Au-mineralizations can be expected with the granitoids. The Mesozoic granitoids are not oxidized enough to have base metal and Mo mineralizations. Sn and W mineralizations and some Ti-Ta-Nb occurrences are possibly associated with reduced granitoids of the Mesozoic age, particularly with the Sn-rich granites.

Acknowledgements: The author (S.O.) is much indebted to Prof. Ochir Gerel and Prof. D. Chuluun (School of Geology, MUST) for their permission to work for mapping (scale 1:50,000) and exploration project in the Hotont area. We are most grateful to Dr. Y. Takahashi for his valuable comments on the original manuscript.

References

Amar-Amgalan (2004) Age determination of Delgerhaan complex. *In* Chuluun, D. and Javkhlanbold, D. (2004).

Blevin, P. L. (2004) Redox and compositional parameters for interpreting granitoid metallogeny of eastern Australia: Implications for gold-rich ore system. *Resource Geol.*, **54**, 241-252.

Chappell, B. W. and White, A. J. R. (1974). Two contrasting granite types. *Pacific Geol.* no. 8, 173-174.

Chuluun, D. and Javkhlanbold, D. (2004) Geological mapping and exploration work using a scale of 1:50,000. *In* Hotont and Tüvshrüüleh sums of Arhangai aimag by Hotont geological party in 2002-2004. Project Report, No. 5595, 393 p. (in Mongolian).

Chuluunsüh, S., Nyamsuren, L. and Altanerdene, L. (1996) Geological mapping using a scale of 1:50,000. *In* Bat-Ölziit sum of Övörhangai aimag in 1994-96. Project Report, No. 4989, 154 p. (in Mongolian).

Collins, W. J., Beams, S. D., White, A. J. R. and Chappell, B. W. (1988) Nature and origin of A-type granites with particular reference to southeastern Australia. *Contrib. Mineral. Petrol.*, **80**, 189-200.

Davaa, Ö., Bayajargal, B. and Ihbayar, Ya. (1996) Geological mapping using a scale of 1:50,000. *In* Bat-Ölziit and Hujirt of Övörhangai aimag, and Tsenher and Tsetserleg sums of Arhangai aimag by Södöt geological party in 1993-95. Project Report No. 5015, 205 p. (in Mongolian).

Ishihara, S. (1971) Modal and chemical compositions of the granitic rocks related to the major molybdenum and tungsten deposits in the Inner Zone of Southwest Japan. *Jour. Geol. Soc. Japan*, **77**, 441-452.

Ishihara, S. (1977) The magnetite series and ilmenite series granitic rocks. *Mining Geol.*, **27**, 293-305.

Ishihara, S., Sato, K. and Terashima, S. (1984) Chemical characteristics and genesis of mineralizaed intermediate-series granitic pluton in the Hobenzan area, western Japan. *Mining Geol.*, **34**, 401-418.

Ishihara, S., Sawata, H., Arpornsuwan, S., Busaracome, P. and Bungrakearti, N. (1979) The magnetite-series and ilmenite-series granitoids and their bearing on tin mineralization, particularly of the Malay Peninsula region. *Geol. Soc. Malaysia, Bull.*, no. 11, 103-110.

Khosbayar, P., Byamba. B. and Binderiya, T. (1987) Geologicheskoye I polesniye iskopayemiye Ogiinuurskogo raiona (Otchyet o resultatah geologosyomochnyh rabot m-ba 1:200,000, provedennykh Ogiinuurskoy partiey v 1985-87), Ulanbaator. Project Report No. 4135, 3 vols., 632 p. (in Russian).

Oyungerel, S., Gerel, O., Chuluun, D., Janchiv, B., Dandar, S. and Tsetseg, R. (2003) Geology and magnetic susceptibility of granitic rocks in the Hotont area, central Mongolia. *Mongolian Geoscientist*, no. 19, 88-90.

Oyungerel, S. and Nyamsuren, Kh. (2003) Petrography of the granitic rocks in the Hotont area, central Mongolia. *MUST, Geology*, no. 9, 115-122.

Pearce, J. A., Harris, N. B. W. and Tindle, A. G. (1984) Trace element discrimination diagrams for the tectonic interpretation of granitic rocks. *Jour. Petrol.*, **11**,

15-32.
Semeikhan, T. and Bold, G. (1970) Geological prospecting report using a scale of 1:200,000. Ulanbaator. Report No. 1831, 180 p. (in Russian).
Tomurtogoo edit. (2004) Terrane map of Mongolia. Scale 1:1,000,000, Geologicaol Information Center (GIC), Mineral Resources Authority of Mongolia (MRAM).
Zen, E-an (1992) Aluminum enrichment in silicate melts by fractional crystallization: some mineralogic and petrographic constraints. *Jour. Petrol.*, **27**, 1097-1117.
Terashima, S. (1974) Spectropotometric determination of chlorine and fluorine in the standard silicate rocks. *Bull. Geol. Surv. Japan*, **25**, 175-179.

Received May 23, 2005
Accepted July 21, 2005

モンゴル中央部，ホトント地域の古生代と中生代の花崗岩類

オユンゲレル サンブー・石原舜三

要　旨

ホトント地域の花崗岩類はバソリス状の後期古生代のデルゲルハーン花崗岩複合体とストック状の前期中生代のエギンダヴァー花崗岩類に２大別される．共に黒雲母花崗岩類を主体とする．デルゲルハーン花崗岩類は低い帯磁率を持ち，その酸素フガシティはQMF付近であり，前期中生代花崗岩類はより還元的で主にチタン鉄鉱系に属する．前期中生代花崗岩類は通常タイプと高スズ花崗岩に分けられ，後者が当地域で最も還元的である．

デルゲルハーン花崗岩類はショショナイト質であるのに対し，エギンダヴァー花崗岩類はショショナイト-高カリウム花崗岩の範疇にプロットされる．両者はハーカー図上で似た傾向を示すが，デルゲルハーン花崗岩類はエギンダヴァー花崗岩類よりもP_2O_5に富み，Fe_2O_3, TiO_2, MgOに乏しい．高スズ花崗岩を除き，そのRb/Srは低く，分化しているとは言えない．これら花崗岩類は島弧環境下の大陸地殻で発生したものと考えられる．高スズ花崗岩は非造山帯環境の大陸地殻内で小規模に発生したマグマと考えられる．

デルゲルハーン花崗岩類には小規模な金鉱化作用が見られるが，この岩体は大規模な貴金属あるいはベースメタル鉱床を伴うには侵食が進み過ぎている．また重要な硫化物鉱床を伴うには，マグマの酸化度，分化指数ともに低すぎる．またエギンダヴァー花崗岩類も硫化物鉱床を伴うには還元的すぎる．むしろ還元的な花崗岩に附随するSn, W, Nb, Taなどの鉱床が期待されるかも知れない．